ORIGINAL ARTICLE

A promising QTL *QSns.sau-MC-3D.1* likely superior to *WAPO1* for the number of spikelets per spike of wheat shows no adverse effects on yield-related traits

Jieguang Zhou[1,2] · Wei Li[1,2] · Yaoyao Yang[1,2] · Xinlin Xie[1,2] · Jiajun Liu[1,2] · Yanling Liu[1,2] · Huaping Tang[1,2] ·
Mei Deng[1,2] · Qiang Xu[1,2] · Qiantao Jiang[1,2] · Guoyue Chen[1,2] · Pengfei Qi[1,2] · Yunfeng Jiang[1,2] · Guangdeng Chen[3] ·
Yuanjiang He[4] · Yong Ren[4] · Liwei Tang[5] · Lulu Gou[6] · Youliang Zheng[1,2] · Yuming Wei[1,2] · Jian Ma[1,2]

Abstract

Key message **A likely new locus *QSns.sau-MC-3D.1* associated with SNS showing no negative effect on yield-related traits compared to *WAPO1* was identified and validated in various genetic populations under multiple environments.**

Abstract The number of spikelets per spike (SNS) is one of the crucial factors determining wheat yield. Thus, improving our understanding of the genes that regulate SNS could help develop wheat varieties with higher yield. In this study, a recombinant inbred line (RIL) population (MC) containing 198 lines derived from a cross between *msf* and Chuannong 16 (CN16) was used to construct a genetic linkage map using the GenoBaits Wheat 16 K Panel. The genetic map contained 5,991 polymorphic SNP markers spanning 2,813.25 cM. A total of twelve QTL for SNS were detected, and two of them, i.e., *QSns.sau-MC-3D.1* and *QSns.sau-MC-7A*, were stably expressed. *QSns.sau-MC-3D.1* had high LOD values ranging from 4.99 to 11.06 and explained 9.71–16.75% of the phenotypic variation. Comparison of *QSns.sau-MC-3D.1* with previously reported SNS QTL suggested that it is likely a novel one, and two kompetitive allele-specific PCR (KASP) markers were further developed. The positive effect of *QSns.sau-MC-3D.1* was also validated in three biparental populations and a diverse panel containing 388 Chinese wheat accessions. Genetic analysis indicated that *WHEAT ORTHOLOG OFAPO1* (*WAPO1*) was a candidate gene for *QSns.sau-MC-7A*. Pyramiding of *QSns.sau-MC-3D.1* and *WAP01* had a great additive effect increasing SNS by 7.10%. Correlation analysis suggested that *QSns.sau-MC-3D.1* was likely independent of effective tiller number, plant height, spike length, anthesis date, and thousand kernel weight. However, the H2 haplotype of *WAPO1* may affect effective tiller number and plant height. These results indicated that utilization of *QSns.sau-MC-3D.1* should be given priority for wheat breeding. Geographical distribution analysis showed that the positive allele of *QSns.nsau-MC-3D.1* was dominant in most wheat-producing regions of China, and it has been positively selected among modern cultivars released in China since the 1940s. Gene prediction, qRT-PCR analysis, and sequence alignment suggested that *TraesCS3D03G0216800* may be the candidate gene of *QSns.nsau-MC-3D.1*. Taken together, these results enrich our understanding of the genetic basis of wheat SNS and will be useful for fine mapping and cloning of the gene underlying *QSns.sau-MC-3D.1*.

Abbreviations

AD	Anthesis date
ANOVA	Analysis of variance
BLUP	Best linear unbiased prediction
CAW	Chinese wheat accession
CMC	Chinese modern cultivar
CS	Chinese Spring
ETN	Effective tiller number
IWGSC	International Wheat Genome Sequencing Consortium
KASP	Kompetitive allele-specific PCR
LY	Luoyang
ML	Mini-core collection
PH	Plant height
PVE	Phenotypic variance
QTL	Quantitative trait loci
RIL	Recombinant inbred line
SL	Spike length
SNP	Single nucleotide polymorphism
SNS	The number of spikelets per spike

Jieguang Zhou and Wei Li have contributed equally to this paper.

Extended author information available on the last page of the article

TKW   Thousand kernel weight
WAPO1   WHEAT ORTHOLOG OFAPO1

Introduction

Bread wheat (AABBDD, *Triticum aestivum* L.) is one of the most important food crops in the world (Liu et al. 2022). The increasing population and frequent natural disasters (Ge et al. 2022) lead to the world confronting a huge food gap, and high yield has always been the eternal theme of wheat breeding. Kernels per spike (KNS), thousand kernel weight (TKW), and spikes per unit area are the three components of yield. The number of spikelets per spike (SNS) is closely related to KNS, and breeders can usually improve wheat yield by increasing SNS. Thus, it is essential to understand the genetic pattern of SNS for optimizing wheat spike structure and cultivating new high-yielding wheat varieties.

To date, quantitative trait loci (QTL) of SNS have been detected on all 21 chromosomes of wheat using bi-parental populations (Singh et al. 2021). For example, Zhai et al. (2016) used a recombinant inbred line (RIL) population to detect a major QTL on chromosome 1B controlling SNS, which explained 30.75% of the phenotypic variance (PVE), and a single nucleotide polymorphism (SNP) marker Kukri _ c8913 _ 655 tightly linked to SNS was identified on chromosome 3D. *QSns.sau-2D* on chromosome 2D significantly increased SNS by up to 14.72% (Ma et al. 2019). Mo et al. (2021) identified two major and novel SNS-related QTL, *QSns.sau-AM-2B.2* and *QSns.sau-AM-3B.2*, using a tetraploid RIL population. Furthermore, some genes related to SNS have been reported, such as *trs1/WFZP-A* (Du et al. 2021), *VRN-A3/FT-A1* (Yan et al. 2006), *Q* (Faris et al. 2003), *TaTB1-4A* (Dixon et al. 2018), *PPD-A1* (Beales et al. 2007), *TaCol-B5* (Zhang et al. 2022), and *WHEAT ORTHOLOG OFAPO1* (*WAPO1*) (Ding et al. 2022; Kuzay et al. 2019). However, the major stably expressed and confirmed QTL for SNS in multiple environments and multiple genetic backgrounds, and high-efficiency molecular markers are still limited.

SNPs are the most abundant and important type of nucleic acid variation (Kharabian-Masouleh et al. 2012). To date, multiple SNP arrays have been developed in wheat, such as the 9 K, 16 K, 55 K, 90 K, 660 K, and 820 K high-density SNP chips. The Wheat 16 K array was developed using an improved genotyping by target sequencing (GBTS) system with capture-in-solution (liquid chip) technology (Guo et al. 2021). The 16 K SNP was identified based on resequencing data from 20 accessions, genotyping data of 1,520 germplasms collected from multiple platforms, and publicly released resequencing and exon capture data. These SNP datasets were developed and optimized using GenoBait

technology to eventually produce 14,868 multiple SNP segments (including 37,669 SNP markers) (Huang et al. 2022).

In this study, we report a genetic map of bread wheat constructed based on the Wheat 16 K SNP array. Using the constructed genetic map, QTL for SNS were identified. Major and novel QTL were validated in four populations with different genetic backgrounds via kompetitive allele-specific PCR (KASP) markers. Furthermore, the genetic effects and geographical distribution of the major QTL were also analyzed to clarify their application potential in breeding and to provide a theoretical basis for genetic improvement of wheat yield.

Materials and methods

Plant materials

The mapping population (MC) containing 198 RILs (F$_6$) was derived from the cross between *msf* and Chuannong 16 (CN16). *msf* is a spontaneous mutant characterized by multi-spikelets, multi-florets, large spike and high fruiting rate (Fig. 1). CN16 is a commercial wheat cultivar, developed by Triticeae Research Institute of Sichuan Agricultural University, with excellent agronomic performances including multiple tillers and good plant architecture (Liu et al. 2018). The MC population was used for QTL identification. Major and novel QTL for SNS identified in the MC RIL population were validated in three populations, including

Fig. 1 Phenotypes of *msf* and CN16. The white bar represents 5 cm

msf × 3642 (M3, F$_3$, and F$_4$, 184 lines), *msf* × 20828 (M2, F$_2$, and F$_3$, 218 lines), and *msf* × Shumai969 (MS9, F$_2$, and F$_3$, 178 lines). The line 20828 was kindly provided by Dr. Wu Yu (Chengdu Institute of Biology, Chinese Academy of Sciences). The line 3642 and cultivar Shumai969 were provided by the Triticeae Research Institute of Sichuan Agricultural University. In addition, three hundred and eighty-eight Chinese wheat accessions (CAW), including 143 landraces from the mini-core collection (ML) and 245 modern cultivars (CMC) released since the 1940s (Table S1), were further employed to verify the effect of the major QTL. The CAW accessions were provided by Dr. Lihui Li (CAAS, China).

Field experiments and phenotypic evaluation

The MC RIL population and parents were planted in five different environments including Wenjiang (103°51′ E, 30°43′ N) in 2021 and 2022 (2021WJ and 2022WJ); Chongzhou (103°38′E, 30°32′N) in 2021 and 2022 (2021CZ and 2022CZ); and Ya'an (103°0′E, 29°58′N) in 2021 (2021YA). The trials in all the environments were performed in a randomized block design with two replications. Seven seeds of each line were planted in a 0.75-m row with 0.1 m between plants, and 0.3 m between rows. Field management followed local practices for wheat production.

SNS was measured by counting the number of spikelets of the main spike, effective tiller number (ETN) was counted as the number of the fertile spike per plant before harvest, plant height (PH) was calculated as the distance from the base to the tip of the highest spike (excluding awns) per plant, spike length (SL) was measured as the length from the rachis node of the first base spikelet to the tip of the main spike (excluding awns) per plant, TKW was calculated as 10 times the average weight of 100 kernels in each line, and anthesis date (AD) was defined as the number of days between sowing and 50% of the plants flowering in each line. At least four plants free of disease in each replicate of each line with consistent growth were selected for trait measurement and then averaged for further analysis.

Three segregation populations for validation, M3, M2, and MS9, were planted in four (2021WJ, 2021CZ, 2022CZ, and 2022YA), two (2021CZ and 2022CZ), and two (2021CZ and 2022CZ) different environments, respectively. CAW was planted in three different environments including Luoyang (Henan province, China) in 2002 and 2005 (2002 LY and 2002 LY), Shunyi (Beijing, China) in 2010 (2010 SY), and Chongzhou (103°38′E, 30°32′N) in 2022 (2022CZ). Planting trials and phenotypic traits collection of CAW (2002 LY, 2005 LY, and 2010 SY) were described by Wang et al. (2019) and Zheng et al. (2014), respectively. The methods of planting and SNS measurement for M3, M2, MS9, and CAW (2022CZ) were same as for the MC RIL population.

Genotyping

Genomic DNA extraction from leaf samples collected at the joining stage adopted the CTAB protocol (Masoodi et al. 2021), and DNA quality was assessed using a NanoDrop One C (Thermo Fisher Scientific, Assembled in the USA). The 198 lines and parents of the MC population were genotyped using the Wheat 16 K SNP array from Mol Breeding Company (Shijiazhuang in Hebei province; http://www.molbreeding.com). The Wheat 660 K SNP array from Capitalbio Technology (Beijing, http://www.capitalbiotech.com/) was also used to genotype the two parents of the MC RIL population. The primers used in this study were synthesized by Tsingke Biotechnology Co., Ltd. (https://www.tsingke.com.cn/).

Data analysis

The frequency distribution of SNS in each environment and correlation analysis were performed using Origin 9.0 software and SPSS V26.0 for Windows (SPSS Inc., Chicago, IL), respectively. The best linear unbiased prediction (BLUP) dataset for all the investigated traits was tested using SAS V8.0 (SAS Institute, Cary, North Carolina). The calculation of the broad-sense heritability (H^2) of SNS was performed as described by Smith et al. (1998). Analysis of variance (ANOVA) was performed using the Aov (ANOVA of multi-environment trials) module of QTL IciMapping V4.1 (https://www.isbreeding.net/) to detect interactions between replications, genotypes, and environments. The Student's *t* test performed by SPSS V26.0 was used to evaluate the differences in parents and RIL population. Furthermore, the correlation coefficients between traits were calculated using SPSS V26.0 based on the BLUP dataset of each trait.

Linkage map construction and QTL analysis

Totally, 37,671 SNP markers (37,669 SNP markers and two polymorphic SNP markers from the 16 K SNP array and the 660 K SNP array, respectively) were obtained. Firstly, the minor allele frequency (MAF) was calculated for each SNP marker in the MC RIL population, and those with MAF greater than 0.3 were retained. Secondly, the retaining markers were analyzed by using the BIN function in QTL IciMapping V4.1, based on their segregation patterns in the MC RIL population, with parameters 'distortion value' and 'missing rate' being set as 0.01 and 20%, respectively. A single marker with the lowest 'missing rate' from each set of bin markers was further selected. Finally, the bin markers were grouped and sorted using the Kosambi mapping function in QTL IciMapping V4.1 with the logarithm of odds (LOD) greater than 3 after preliminary analysis of markers with LOD scores ranging from 2 to 10. The finally

retained markers were used to generate genetic maps using the 'MAP' function in the QTL IciMapping V4.1 software and maps were further drawn in MapChart V2.32. The flanking sequences (200 bp) of SNPs were used to blast against (E-value of $1e^{-5}$) genome sequences of the International Wheat Genome Sequencing Consortium (IWGSC) Chinese Spring (CS) RefSeq V2.1 (Zhu et al. 2021) to get their physical locations. The syntenic relationships between the genetic and physical maps of the bin markers were presented using the Strawberry Perl V5.24.0.1.

Inclusive composite interval mapping with the biparental population module (mapping method: ICIM-ADD. Step = 1 cM, PIN = 0.001, and LOD threshold = 2.5) in QTL IciMapping V4.1 was performed to detect QTL for SNS. These QTL, which were detected in more than three environments (including BLUP dataset) and explained greater than 10% of the PVE, were considered as major and stable QTL, and those with common flanking markers were treated as identical ones.

The detected QTL were basically named as per the International Rules of Genetic Nomenclature (http://wheat.pw. usda.gov/ggpages/wgc/98/Intro.htm). 'Q,' 'SNS,' 'sau,' and 'MC' represent 'QTL,' 'the number of spikelets per spike,' 'Sichuan Agricultural University,' and 'the MC RIL population,' respectively.

Comparison with previously reported QTL/SNP for SNS

Previously reported closely linked marker sequences of QTL/SNP related to SNS were obtained from WheatQTLdb V2.0 (Singh et al. 2021), and further blasted against genomes sequences of IWGSC RefSeq V2.1 (Zhu et al. 2021) to get their physical locations.

Marker development and QTL validation

To further narrow down the intervals of major QTL, two SNP markers, from the 660 K SNP array, showing polymorphism in the parents were converted into KASP markers (Table S2) to genotype the MC RIL population. According to QTL mapping results, the flanking markers closely linked to novel and major QTL were converted to KASP markers, and the method of KASP development was consistent with the description of Liu et al. (2018). The validation populations, M3, M2, MS9, and CAW, were genotyped using the KASP marker (Table S2). The 10-μl reaction system includes 1-μl DNA, 2.6-μl RNA-free deionized water, 5-μl SsoFast Eva-Green mixture (Bio-Rad, Hercules, CA, USA), and 1.4-μl of mixture forward and reverse primers. All KASP processes were carried out on a CFX96 Real-Time PCR Detection System (BioRad, USA) (Li et al. 2020a). The lines were divided into two groups based on the genotyping results:

(1) lines with homozygous genotype GG from *msf*; (2) lines with homozygous genotype AA from alternative parent. The difference between the two groups was calculated as: The ratio of the phenotypic value difference between the GG lines and the AA lines to that of the AA lines. Finally, we assessed the differences in SNS between the three groups using an independent samples t test ($P < 0.05$) to determine the effects of major QTL.

Identification of 1BL/1RS translocation

The parental CN16 is a genotype carrying the 1BL/1RS translocation (Liu et al. 2018). Thus, we identified 1BL/1RS translocations of the RILs derived from *msf* and CN16. Firstly, SNP markers on chromosome 1B were screened from the 16 K SNP array in the MC RIL population (2,061 markers in total). The markers mapped on 1BS of IWGSC RefSeq V2.1 (Zhu et al. 2021) were identified (501 markers). Secondly, SNP markers genotyped as 'NA' (no genotype detected) in CN16 were retained (276 markers) for further analysis. The 'NA' information present under 276 markers for each line was counted. According to the distribution of NA in each line, the lines with less than or equal to 19 NA in these 276 markers were considered as non-1BL/1RS translocation lines and those with the number of NA greater than or equal to 62 were 1BL/1RS translocation lines. Moreover, to validate the 1BL/1RS translocation in the MC RIL population, we also used the 1BS- and 1RS-specific markers to detect the translocation (Jung and Seo 2021). The 20-μl reaction system included 2-μl DNA, 6-μl RNA-free deionized water, 10-μl 2 × Taq PCR PreMix (+ Blue dye, innovagene), and 1 μl of each primer (10 μm). The reaction conditions were as follows: pre-denaturation at 95 ℃ for 5 min; a total of 35 cycles of denaturation at 95 ℃ for 30 s, annealing at 62 ℃ for 30 s and extension at 72 ℃ for 30 s; and final extension at 72 ℃ for 7 min. Primer information was listed in Table S2. Finally, the lines carrying 1BL/1RS translocation from the MC RIL population were counted based on the above two methods.

Potential candidate gene(s) for major QTL

According to the mapping result, the sequences of the flanking markers were used to blast (E-value of $1e^{-5}$) against the IWGSC RefSeq V2.1 to obtain their physical locations. The high-confidence genes within the physical positions were obtained from WheatOmics 1.0 (http://202. 194.139.32/) (Ma et al. 2021). The functional annotations of predicted genes were assigned based on UniProt (http://www.uniprot.org/). Gene expression data in various tissues was extracted from expVIP (http://www.wheat-expression. com/). The data on gene expression patterns in different stages of spike development were obtained from a previous

study (Li et al. 2018). Furthermore, the expression pattern of the predicted gene was represented in the HeatMap drawn on Hiplot (Li et al. 2022). The whole genome resequencing of the two parents was performed by Haorui Company (Xian, China) based on PacBio®HiFi sequencing platform. Genomic sequences for the candidate gene, including the coding region sequence (CDS) and the 2000-bp upstream promoter sequence (P2000), were obtained from the resequencing data of the two parents (unpublished) and then aligned to identify sequence polymorphism.

Gene expression studies

Total RNA extracted from freshly harvested spikes at single ridge end-stage with the RNAprep pure Plant Kit (Biofit Biotechnologies co. Ltd, Chengdu, China) was digested with RNase-free DNase (Takara) to remove residual genomic DNA. The RNA was reverse-transcribed into cDNA by using a Prime ScriptTM RT Reagent Kit (TaKaRa, Kyoto, Japan) according to the manufacturer's instructions. SYBR qPCR Master Mix kit (Q711, Vazyme, Nanjing, China) and a Bio-Rad CFX96 real-time PCR detection system (Bio-Rad, Hercules, USA) were used for qRT-PCR. Three biological replicates were performed for each parent, and each sample was assayed three times. The PCR reaction mixture contained: 2-µl cDNA, 5-µl 2X SYBR Green mix, 0.5-µl forward primer, 0.5-µl reverse primer, and 2-µl ddH$_2$O, in a final volume of 10 µl. The PCR program was as follows: 94 °C for 5 min, followed by 35 cycles of 94 °C for 30 s, 62 °C for 30 s, and finally 72 °C for 30 s. The $2^{-\Delta\Delta Ct}$ method was used to calculate the relative expression levels of the candidate genes. The actin gene was used as an internal control. Specific primers for qRT-PCR were designed in NCBI, and the details of primers are listed in Table S2.

Results

Linkage map construction

Of the 37,671 SNPs, 5,991 (~ 15.90%) with MAF ≥ 0.3 and showing polymorphisms between parents in the MC mapping population were retained for further analysis. These 5,991 SNP markers were divided into 1,150 bins using the 'BIN' function in QTL IciMapping V4.1, and markers with the lowest 'missing rate' in each bin (bin markers) were selected and used to construct the genetic map (Table 1). The resultant linkage map consisted of 1,150 bin markers which were classified into 26 linkage groups (Table 1). Among them, chromosomes 3D, 4A, 5A, 5D, and 7B each had two linkage groups, and only one was constructed for each of the remaining chromosomes (Table 1). Chromosome arm 1BS was not covered by any marker mainly due

to the 1BL/1RS translocation on chromosome 1B (Fig. 2). The total length of the 26 linkage groups was 2,813.25 cM, with an average spacing of 2.45 cM (Table 1). The A, B, and D genomes included 479 (~ 41.65%), 473 (~ 41.13%), and 198 (~ 17.22%) markers covering lengths of 1,047.05, 925.92, and 840.28 cM with average marker intervals of 2.19, 1.96, and 4.24 cM, respectively (Table 1). The lowest marker coverage was detected for the D genome, especially for chromosomes 4D and 6D (Table 1).

Comparison of genetic and physical maps

The sequences of the 5,991 mapped markers were blasted against CS V2.1 genome to obtain their physical positions (Table S3). Among them, 5980 markers (99.82%) showed coincident physical and genetic positions (Table S3). The genetic positions of the 1,150 bin markers were compared with their physical positions in the CS V2.1 genome, and 1,015 (~ 88.26%) markers showed good concordance (Fig. 2 and Table S4).

Phenotypic variation and ANOVA analysis

msf had a higher value of SNS than CN16 (Fig. 1, $P < 0.01$) in five environments (Table 2). The SNS of the MC RIL population ranged between 14.00 and 29.00 and was normally and continuously distributed (Fig S1 and Table 2), indicating polygenic control. The estimated H^2 of SNS was 0.74, indicating that SNS was significantly affected by genetic factors (Table 2). ANOVA showed a significant effect of G (Genotype), E (Environment), and G × E interaction on SNS ($P < 0.001$; Table S5). However, Block/E did not differ significantly ($P > 0.05$) on SNS (Table S5), suggesting that two planting replicates within a single environment were reliable and meaningful.

Correlation analyses between SNS and other agronomic traits

SNS showed a significant and positive correlation ($P < 0.01$) in all five environments and BLUP dataset (Fig. 3), with coefficients ranging from 0.32 and 0.79 (Fig. 3). The BLUP dataset of SNS and five other agronomic traits were used to evaluate their Pearson's correlations. There was a significant correlation between SNS and SL, AD, and TKW (Table 3). Furthermore, there was no significant correlation between SNS and ETN, and PH (Table 3).

Identification of QTL for SNS

Twelve QTL for SNS were identified, and they were located on chromosomes 1B, 2A, 3D (2), 4A, 5A, 5B (2), 6A, 6B, 7A, and 7B, with LOD scores ranging between 2.52 and

Table 1 Details of the linkage maps

Chromosome	Group	Number of bin marker	Number of mapped markers	Length (cM)	cM per bin marker
1A	1	78	546	131.19	1.68
2A	1	77	297	148.17	1.92
3A	1	84	439	185.41	2.21
4A	2	57	318	147.74	2.59
5A	2	84	362	161.7	1.92
6A	1	48	327	141.65	2.95
7A	1	51	171	131.2	2.57
A genome	9	479	2460	1047.05	2.19
1B	1	47	557	93.11	1.98
2B	1	77	414	209.96	2.73
3B	1	74	427	145.19	1.96
4B	1	46	169	122.34	2.66
5B	1	64	258	137.45	2.15
6B	1	77	751	84.71	1.1
7B	2	88	313	133.16	1.51
B genome	8	473	2,889	925.92	1.96
1D	1	37	150	119.24	3.22
2D	1	31	132	104.03	3.36
3D	2	41 (43)	99 (101)	148.94 (250.45)	3.63 (5.82)
4D	1	23	69	54.55	2.37
5D	2	29	78	153.05	5.28
6D	1	7	41	60.91	8.7
7D	1	28	71	98.05	3.5
D genome	9	196 (198)	640 (642)	738.77 (840.28)	3.77 (4.24)
Total	26	1148 (1150)	5989 (5991)	2711.74 (2813.25)	2.36 (2.45)

The values in parentheses were the reconstruction result of the linkage genetic map on chromosome 3D

16.66 (Table 4). Among them, *QSns.sau-MC-3D.1* and *QSns.sau-MC-7A* were identified in three and five environments as well as using the BLUP dataset (Table 4), respectively. In addition, *QSns.sau-MC-3D.1* and *QSns.sau-MC-7A* explained 9.71–16.75% (average = 14.41%) and 8.95–24.25% (average = 16.18%) of PVE, respectively (Table 4). Therefore, these two QTL were considered as the major and stable QTL for SNS. The remaining eight QTL were detected in a single or two environments explaining between 3.21% and 9.61% of the PVE, and they were accordingly designated as minor QTL (Table 4). The positive alleles of *QSns.sau-MC-3D.1* and *QSns.sau-MC-7A* were both derived from the parent *msf*.

QSns.sau-MC-3D.1 was located in a 20.04-Mb region between 3D_44252198 and 3D_64273412 (Fig. 4A). The 660 K SNP array was used to genotype the two parents of the MC RIL population, and two KASP markers were further developed in this region (Table S2). The linkage genetic map on chromosome 3D was reconstructed and QTL for SNS were remapped. Finally, *QSns.sau-MC-3D.1* was located in an 8-cM (10.79-Mb) region between KASP-10

and 3D_64273412. It explained 9.71–16.75% of the PVE (Table 4). The effect of *QSns.sau-MC-3D.1* was highly significant ($P < 0.01$) in five environments and BLUP dataset (Fig. 4B). According to flanking marker profiles of *QSns.sau-MC-3D.1*, lines with the homozygous genotype GG from *msf* had significantly higher ($P < 0.01$) SNS than those with the homozygous genotype AA from CN16 and the difference ranged from 2.29 to 6.94% (Fig. 4B). Therefore, this QTL was considered as a major one.

QSns.sau-MC-7A was stably detected in all environments and located in a 9-cM region between 7A_671413788 and 7A_673311365 (Table 4). It can explain up to 24.25% of the PVE (Table 4). *QSns.sau-MC-7A* was located between 676.01 and 679.91 Mb on CS 7AL by anchoring flanking markers 7A_671413788 and 7A_673311365 (Table 4). Here, it is worth noting that *WAPO1* (*TraesCS7A03G1166400*) is also located in this interval (Kuzay et al. 2019). According to our previous study by Ding et al. (2022), *WAPO1* was classified into four haplotypes, including H1 ($140^G + 115^{deletion}$), H2 ($140^T + 115^{insertion}$), H3 ($140^G + 115^{insertion}$), and H4

Fig. 2 Syntenic relationships between the genetic and physical maps of bin markers. GM-1A to GM-7D represented the 26 chromosomal genetic maps used in this study; PM-1A to PM-7D represented the 21 chromosomal physical maps of wheat
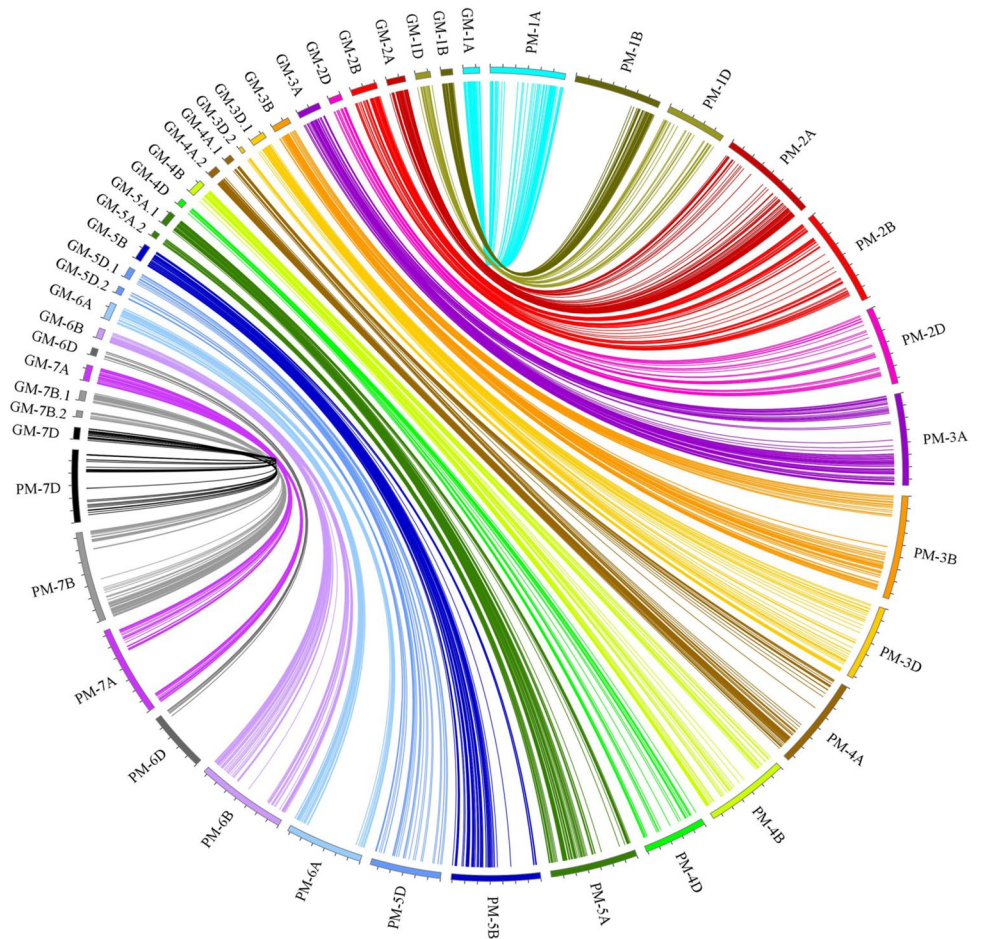
Table 2 Phenotypic variation of the number of spikelets per spike (SNS) for the mapping population in five environments and BLUP

Env	Parents		$msf \times$CN16			
	msf	CN16	Min–Max	Mean	SD	H^2
2021WJ	27.60**	20.00	19.00–26.75	23.08	1.64	0.74
2021CZ	25.50**	20.44	19.00–25.88	22.78	1.26	
2021YA	27.67**	22.00	18.00–29.00	23.45	1.97	
2022WJ	24.00**	18.13	17.14–26.00	21.06	1.58	
2022CZ	24.17**	19.00	14.00–28.00	21.35	2.09	
BLUP	25.12**	20.30	19.89–24.42	21.85	0.96	

Env., Environment

**Significance level at $P < 0.01$; SD, standard deviation; H^2, broad-sense heritability; WJ, Wenjiang; CZ, Chongzhou; YA, Ya'an; BLUP, best linear unbiased prediction

($140^T + 115^{deletion}$), based on the types of SNP in its F-box region and an insertion/deletion fragment in the promoter sequence. Hence, we used the previously reported functional marker (K-WAPO1) and InDel marker (WAPO1-ProS) of *WAPO1* to genotype *msf* and CN16 (Table S2). Genotyping results showed that *msf* and CN16 belong to H2 and H3, respectively (Fig S2). This result is consistent with the previous result that H2 is an excellent haplotype that can increase SNS (Ding et al. 2022), and further suggests that *WAPO1* is likely the causal gene for *QSns.sau-MC-7A*. Furthermore, the MC RIL population was divided into two groups (lines with haplotypes H2 and H3, respectively) based on the genotyping result of K-WAPO1. SNS of the group with H2 had significantly ($P < 0.01$) greater values than that with H3 in each environment and BLUP dataset (Fig S3B).
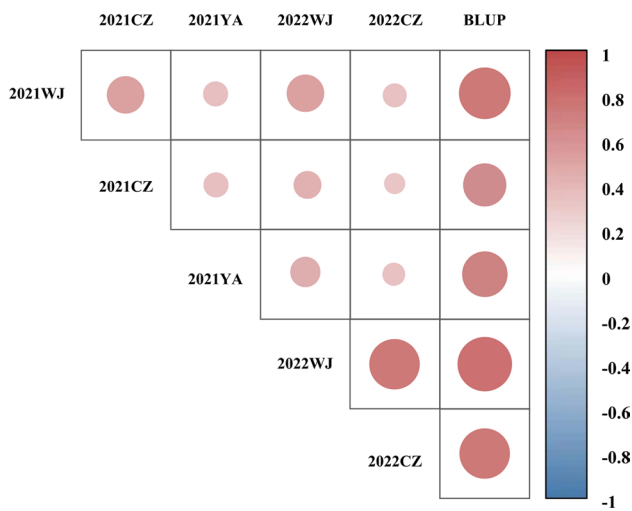
Fig. 3 Correlation coefficients of the number of spikelets per spike (SNS) in multiple environments. All 'correlation coefficient' showed significant level at $P < 0.01$

Table 3 Correlations between the number of spikelets per spike (SNS) and other agronomic traits in the mapping population

Trait	Correlation coefficients
Effective tiller number (ETN)	− 0.036
Plant height (PH)	0.086
Spike length (SL)	0.35**
Anthesis date (AD)	0.40**
Thousand kernel weight (TKW)	− 0.14*

*Significance level at $P < 0.05$; **significance level at $P < 0.01$

Validation of *QSns.sau-MC-3D.1*

The effects of *QSns.sau-MC-3D.1* were further evaluated in four additional populations with different genetic backgrounds (M3, M2, MS9, and CAW) using the newly designed KASP marker KASP-10 (Table S2) tightly linked to *QSns.sau-MC-3D.1*. Genotyping was executed for 184, 218, 178, and 388 lines of the M3, M2, MS9, and CAW populations, respectively (Fig S4).

The M3 population was planted in four different environments. In all the four environments, the group with the homozygous genotype GG from *msf* had significantly greater SNS than that with the homozygous genotype AA ($P < 0.01$), and the differences between the two groups were 4.13%, 3.59%, 4.90%, and 3.84%, respectively (Fig. 5A). The M2 population was planted in two different environments. In both environments, lines with the homozygous genotype GG from *msf* had significantly higher SNS than those with AA ($P < 0.01$), and the differences between the two groups were 9.31%, and 4.74%, respectively (Fig. 5B).

Likewise, the MS9 population was planted in two different environments. Group 1, with the homozygous genotype GG from *msf*, had a significantly ($P < 0.01$) higher SNS than group 2 (with the homozygous genotype AA) in the two environments with differences of 6.01% and 7.60%, respectively (Fig. 5C). In the CAW population, the group with the homozygous genotype GG showed significantly higher SNS than that of the homozygous genotype AA ($P < 0.05$, Fig. 5D). The above results indicate that *QSns.sau-MC-3D.1* is a major QTL controlling SNS.

Effects of *QSns.sau-MC-3D.1* and *WAPO1* on increasing SNS

The effects of *QSns.sau-MC-3D.1* and *WAPO1* on increasing the SNS were further evaluated (Fig. 6). Compared with the lines without any of the positive alleles increasing SNS, those only possessing the positive allele GG of *QSns.sau-MC-3D.1* or H2 of *WAPO1* significantly ($P < 0.01$) increased SNS by 2.61% and 3.54%, respectively. And those with the combination of positive alleles of both *QSns.sau-MC-3D.1* and H2 significantly ($P < 0.01$) increased SNS by up to 7.10% (Fig. 6). In addition, lines with the combination of positive alleles of *QSns.sau-MC-3D.1* and H2 significantly ($P < 0.01$) increased SNS by 4.37 and 3.44%, respectively, compared to those with either positive allele of *QSns.sau-MC-3D.1* or H2 (Fig. 6). However, there was no significant difference between the lines with *QSns.sau-MC-3D.1* and H2 (Fig. 6), indicating that the genetic effect between *QSns.sau-MC-3D.1* and *WAPO1* may be additive.

Correlation between major QTL and other agronomic traits

The lines carrying H2 of *WAPO1* in the MC RIL population were removed, and the remaining lines were used to detect correlations between *QSns.sau-MC-3D.1* and other yield-related traits. The remaining lines were divided into two groups: lines with the homozygous genotype from *msf* (GG, 42 lines) or CN16 (AA, 48 lines) based on genotyping results using KASP-10 (Fig. 7). There were no significant differences ($P > 0.05$) between the two groups for any of the yield-related traits (ETN, PH, SL, AD, and TKW), suggesting that the expression of *QSns.sau-MC-3D.1* was likely independent of these agronomic traits (Fig. 7). Similarly, the lines that did not carry the homozygous genotype GG of *QSns.sau-MC-3D.1* were divided into two groups: lines with the H2 (41 lines) or H3 (48 lines) based on genotyping results with K-WAPO1 (Fig. 7). There were significant differences between the two groups in ETN and PH (Fig. 7), indicating that H2 haplotype of *WAPO1* may affect ETN and PH.

Table 4 Quantitative trait loci for the number of spikelets per spike (SNS) identified in the mapping population evaluated in five environments and BLUP

QTL	Env	Interval (cM)	Flanking marker	LOD	PVE (%)	Add	Physical position (Mb)
QSns.sau-MC-1B	2021CZ	84.5–93	1B_679421143 and 1B_687066854	2.65	4.26	− 0.27	688.30–696.94
QSns.sau-MC-2A	BLUP	53.5–64.5	2A_144065493 and 2A_165841608	2.52	3.21	0.18	148.72–170.38
QSns.sau-MC-3D.1	2021YA	81.5–89.5	KASP-10 and 3D_64273412	7.2	16.75	0.82	53.61–64.40
	2022WJ	83.5–88.5	KASP-10 and 3D_64273412	9.71	14.82	0.62	
	2022CZ	81.5–88.5	KASP-10 and 3D_64273412	4.99	9.71	0.63	
	BLUP	83.5–88.5	KASP-10 and 3D_64273412	11.06	16.34	0.4	
QSns.sau-MC-3D.2	2021WJ	96.5–100.5	3D_122396589 and 3D_138793245	3.05	5.32	0.38	122.97–139.28
QSns.sau-MC-4A	2022WJ	29.5–35.5	4A_639942192 and 4A_679248111	6.31	9.61	0.5	639.38–681.19
	2022CZ	29.5–35.5	4A_639942192 and 4A_679248111	4.41	8.47	0.60	
	BLUP	28.5–35.5	4A_639942192 and 4A_679248111	2.95	3.85	0.19	
QSns.sau-MC-5A	2022WJ	0–13.5	5A_9510718 and 5A_27776458	2.57	4.42	0.34	11.56–29.72
QSns.sau-MC-5B.1	2021WJ	9.5–17.5	5B_38648213 and 5B_43372176	3.48	6.16	0.41	39.68–230.88
	BLUP	10.5–19.5	5B_43372176 and 5B_227699843	3.45	5.06	0.22	
QSns.sau-MC-5B.2	2021CZ	24.5–25.5	5B_401661494 and 5B_414921497	2.85	4.59	0.28	404.64–417.83
QSns.sau-MC-6A	2022WJ	0–5.5	6A_3774779 and 6A_5558438	3.16	4.37	0.34	4.57–6.86
QSns.sau-MC-6B	2022CZ	23.5–24.5	6B_644045066 and 6B_647440241	2.99	5.34	− 0.47	652.23–655.69
QSns.sau-MC-7A	2021WJ	100.5–107.5	7A_671413788 and 7A_672390144	7	12.85	0.59	676.01–679.91
	2021CZ	105.5–108.5	7A_671413788 and 7A_672390144	12.28	22.42	0.61	
	2021YA	107.5–109.5	7A_672390144 and 7A_673311365	7.32	15.87	0.8	
	2022WJ	100.5–107.5	7A_671413788 and 7A_672390144	8.55	12.71	0.57	
	2022CZ	101.5–107.5	7A_671413788 and 7A_672390144	4.97	8.95	0.61	
	BLUP	105.5–107.5	7A_671413788 and 7A_672390144	16.66	24.25	0.49	
QSns.sau-MC-7B	2021WJ	73.5–80	7B_582312831 and 7B_587920157	2.77	4.79	0.36	586.93–592.64

QTL quantitative trait loci; *Env.* environment; *BLUP* best linear unbiased prediction; *LOD* logarithm of odds; *PVE* phenotype variance explained. *Add* additive effect (positive values: positive alleles from *msf*, negative values: positive alleles from CN16). Physical position, the flanking marker sequences of QTL were blasted against IWGSC RefSeq V2.1 to get physical positions

QSns.sau-MC-3D.1 underwent positive selection in artificial domestication and breeding

In order to comprehensively and systematically evaluate the distribution of *QSns.sau-MC-3D.1* in Chinese wheat accessions, three hundred and eighty-eight accessions of the CAW population were genotyped using KASP-10. According to the polymorphism of KASP-10, the accessions were divided into two groups in the CAW population: accessions with the homozygous genotype GG and those with AA (excluding heterozygous genotype GA).

In ML, the homozygous genotype GG of *QSns.sau-MC-3D.1* was dominant in all seven wheat zones except III (23.53%), V (33.33%), and VII (20%, Fig S5A). The CMC population was used to further reveal the *QSns.sau-MC-3D.1* distribution in China. As shown in Fig S5B, the frequency of homozygous genotype GG for *QSns.sau-MC-3D.1* was dominant in almost all zones except the V zone (12.5%). I, II, and III belong to the zones with the oldest and strongest wheat breeding programs in China (Zheng et al. 2014). It is worth noting that the average frequency of homozygous genotype GG at *QSns.sau-MC-3D.1* in zones I (66.67%), II (86.57%), and III (65%) was 72.74% (Fig S5A), which was much higher than that in ML (62.68%, Fig S5B), suggesting that modern breeding has greatly increased its frequency in CMC. Furthermore, in ML, there was no significant difference in SNS between the group with GG and that with AA (Fig S5C). In CMC, the group with GG had significantly higher SNS (1.58%, $P < 0.05$) than that with AA (Fig S5D). This suggests breeders may have indirectly increased the frequency of genotype GG of *QSns.sau-MC-3D.1* in modern breeding by selecting genotypes with higher SNS.

SNS is not affected by 1BL/1RS translocation

In the current study, CN16 is a cultivar with 1BL/1RS translocation. Identification of 1BL/1RS translocations in the MC RIL population revealed 58 lines carrying 1BL/1RS translocations, while 116 not (Fig S6). *t* test showed there was no significant ($P > 0.05$) difference between the SNS of the two groups (Fig S6), suggesting that 1BL/1RS translocations may not affect SNS in the MC RIL population.
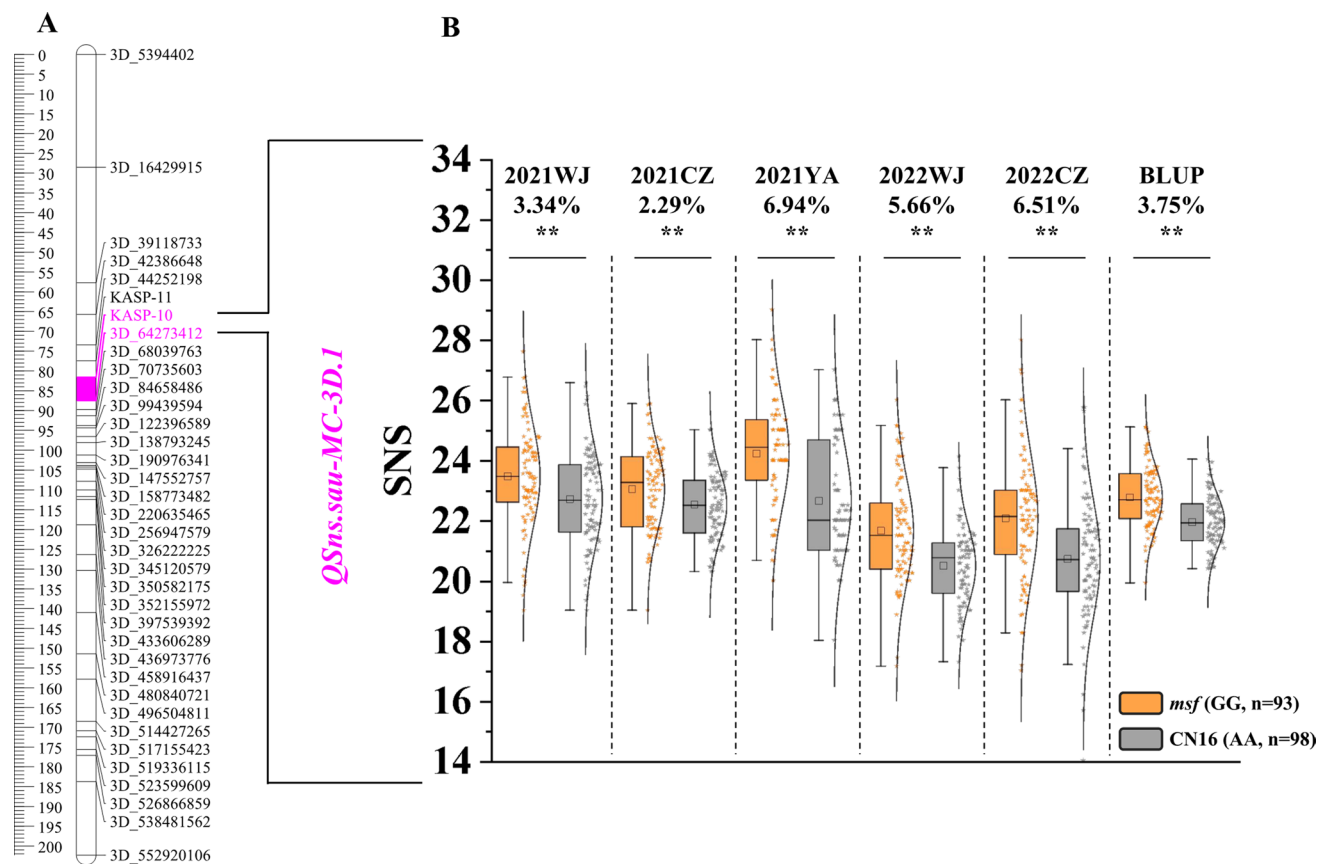
Fig. 4 Genetic map of the major *QSns.sau-MC-3D.1* and its effect. **A** Genetic map of chromosome 3D. The red area is the interval of *QSns.sau-MC-3D.1*. **B** A box plot that shows the effect of *QSns.sau-MC-3D.1* calculated after grouping the MC RIL population into two categories based on the genotypes of flanking markers. Orange and gray boxes indicate lines with the homozygous genotype from *msf* (GG) and CN16 (AA), respectively. **Significance level at $P < 0.01$, ns indicates no significant difference between the two groups. Differences in SNS between the two groups are labeled below the environment names and BLUP

Prediction of candidate gene(s)

There were 93 high-confidence genes within the interval of *QSns.sau-MC-3D.1* (53.61–64.40 Mb, Table S6). Their expression patterns in various tissues and spikes at different developmental stages were analyzed. The results showed that there were nine genes greatly expressed in spike at the reproductive stage and seven genes highly expressed in spike at the single and double ridge stage with two genes shared (Fig S7), suggesting that these two genes might be involved in spike development. *TraesCS3D03G0222600* and *TraesCS3D03G0216800* encoding MYB-like transcription factor and basic helix-loop-helix (HLH) transcription factor, respectively, were likely related to spike development based on gene annotation (Table S6). qRT-PCR analysis further suggested that only the expression level of *TraesCS3D03G0216800* was significantly enhanced in *msf* ($P < 0.05$, Fig S8). We further analyzed the P2000 and CDS of *TraesCS3D03G0216800* based on the parental resequencing data of the MC RIL population. For the P2000, a total of

12 SNPs were detected in *TraesCS3D03G0216800* between *msf* and CN16, including one SNP insertion (at position 1902 bp-T/ins) and 11 SNP deletions (at positions 97-C/del, 383-G/del, 629-T/del, 1184-A/del, 1304-T/del, 1379-T/del, 1402-T/del, 1739-G/del, 1767-C/del, 1821-G/del, and 1974 bp-A/del, Table S7). For the CDS, there were eight SNPs including one SNP insertion (at position 207 bp-C/ins), two SNP substitutions (at position 744 bp-GT/AG), and five SNP deletions (at positions 223-G/del, 556-C/del, 742-CA/del, and 835 bp-C/del, Table S7). Taken together, our results suggested that *TraesCS3D03G0216800* may play a regulatory role in determining SNS.

Discussion

Phenotypic correlations among investigated traits

In this study, SNS was significantly and positively correlated with SL (Table 3), being consistent with previous
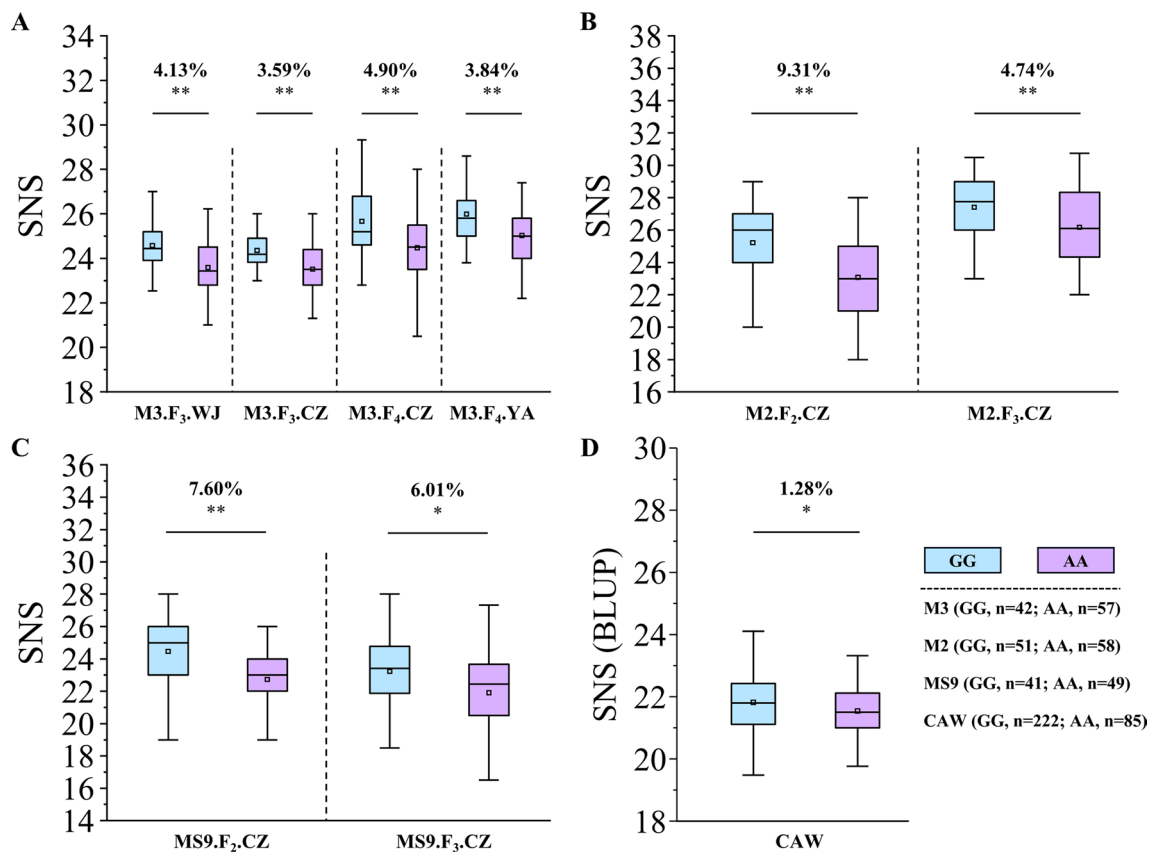
Fig. 5 Validation of *QSns.sau-MC-3D.1* in four populations. **A–D** Effects of *QSns.sau-MC-3D.1* in the four validation populations (i.e., *msf* × 3642, *msf* × 20828, *msf* × Shumai969, and CAW). Lines with the homozygous genotype GG of *msf* × 3642, *msf* × 20828, *msf* × Shumai969, and CAW population are 42, 51, 41, and 222, respectively. Lines with homozygous genotype AA of *msf* × 3642, *msf* × 20828, *msf* × Shumai969, and CAW population are 57, 58, 49, and 85, respectively. *Significance level at $P < 0.05$, **Significance level at $P < 0.01$. Percentage differences between the two groups are indicated above the P values at the top of each plot

studies (Che et al. 2018), suggesting that longer SL provides room for more spikelets to grow (Ding et al. 2011). There was a significant positive correlation between SNS and AD (Table 3). This result with previous studies indicated that plants with a longer flowering time may have more time for the differentiation and development of the spikelet primordia (Boden et al. 2015). Moreover, SNS was significantly and negatively correlated with TKW (Table 3). Considering the source reservoir relationship in the plant, the increase in the number of spikelets may lead to a decrease in the nutrients allocated to a single kernel (Che et al. 2018). These results provide a vital basis for understanding the complex relationships among various traits to further improve wheat yield.

QSns.sau-MC-3D.1 is a novel QTL for SNS

Physical locations of the QTL/SNP for SNS in previous studies and *QSns.sau-MC-3D.1* were compared (Fig S9). *QSns.sau-MC-3D.1* was located between 53.61 and 64.40 Mb in the deletion bin 3DS6-0.55–1.00 on chromosome arm 3DS in CS (Fig S9A and B), which was different from the

previously reported SNS-related QTL/SNP (Fig S9C). For example, *QTsn.cau-3D.3* was located at 3.99 Mb on chromosome arm 3DS with the peak marker CAP11_c3914_325 (Zhai et al. 2016). *QTL1935* was physically located on chromosome arm 3DS at 110.04–129.55 Mb, overlapping with *QSns.cd-3D* (Chen et al. 2017). Two SNS-related SNPs, T/C (Zhai et al. 2016) and C/T (Sun et al. 2017), were located at 512.68 Mb and 600.26 Mb, respectively, on chromosome arm 2BL. Comparison of the physical locations of *QSns.sau-MC-3D.1* with those of previously reported QTL suggests that *QSns.sau-MC-3D.1* is likely a novel QTL controlling SNS (Fig S9C).

The yield improvement potential of *QSns.sau-MC-3D.1* is likely superior to that of *WAPO1*

Here, two major and stably expressed QTL, *QSns.sau-MC-3D.1* and *QSns.sau-MC-7A* (*WAPO1*), for SNS were identified. Both the positive allele of *QSns.sau-MC-3D.1* and the H2 haplotype of *WAPO1* significantly ($P < 0.01$) increased SNS (Fig. 4 and Fig S3). SNS was reported to be negatively
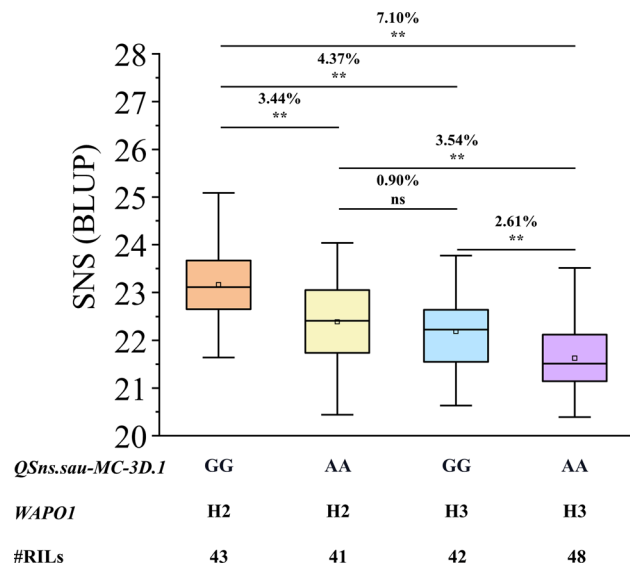
Fig. 6 Additive effects of *QSns.sau-MC-3D.1* and *WAPO1* on increasing SNS. 'H2' and 'H3' represented the H2 ($140^T + 115^{insertion}$) and H3 ($140^G + 115^{insertion}$) haplotype of *WAPO1*, respectively. **Significance level at $P < 0.01$, and ns indicates no significant difference between the two groups. Percentage differences between the two groups are indicated above the P values at the top of each plot

correlated with ETN and TKW (Ma et al. 2019), and positively with PH and AD (Mo et al. 2021), suggesting it is not conducive to yield improvement. Here, the expression of *QSns.sau-MC-3D.1* was independent of the above agronomic traits (Fig. 7). However, H2 haplotype expression of *WAPO1* may affect ETN and PH (Fig. 7). Furthermore, *QSns.sau-MC-3D.1* underwent positive selection in modern breeding (Fig S5B and D). Thus, *QSns.sau-MC-3D.1* may have a promising breeding potential.

Candidate gene analysis of *QSns.sau-MC-3D.1*

According to the CS reference genome, there were 93 annotated high-confidence genes within the candidate interval of *QSns.sau-MC-3D.1* (Table S6). Spatiotemporal expression patterns and functional annotations of these genes suggested that two genes, *TraesCS3D03G0222600* and *TraesCS3D03G0216800* may be involved in determining the development of SNS (Fig S7, Table S6). Previous studies have also shown that MYB transcription factors determined the fate of spikelet meristem (Li et al. 2020b; Seetharam et al. 2021), and HLH transcription factor regulated flowering time in grasses (Zhao et al. 2011). However, qRT-PCR of the two genes showed that only *TraesCS3D03G0216800* was differentially expressed between parents. A number of sequence variations in
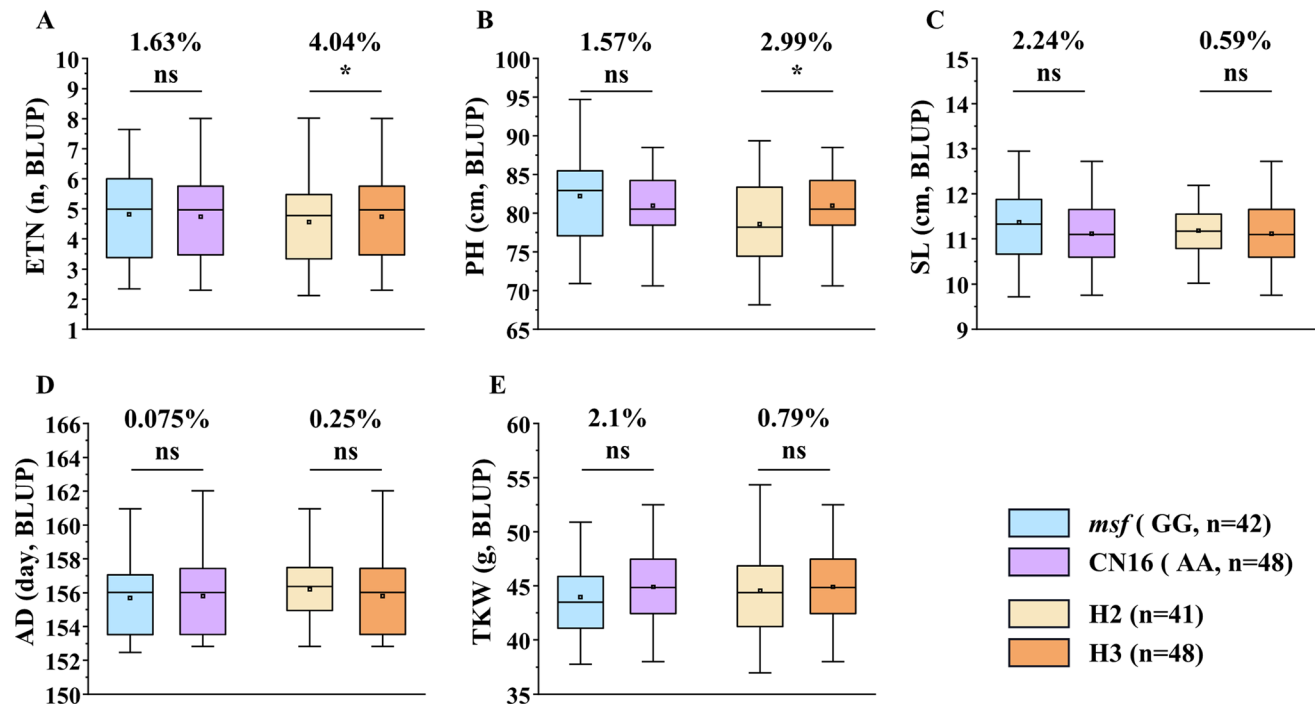
Fig. 7 Effects of two major QTL (*QSns.sau-MC-3D.1* and *WAPO1*) on other agronomic traits. **A** Effective tiller number (ETN); **B** Plant height (PH); **C** Spike length (SL); **D** Anthesis date (AD); **E** Thousand kernel weight (TKW); *Significance level at $P < 0.05$, ns indicates no significant difference between the two groups. Percentage differences between the two groups are indicated above the P values at the top of each plot

promoter and CDS of *TraesCS3D03G0216800* between parents were detected (Table S7). These results suggested that *TraesCS3D03G0216800* may be a candidate gene for *QSns.sau-MC-3D.1*.

Conclusion

In this study, we identified two major QTL (*QSns.sau-MC-3D.1* and *QSns.sau-MC-7A*) in a RIL population. *WAPO1* was demonstrated to be the candidate gene for *QSns.sau-MC-7A*. *QSns.sau-MC-3D.1* was a novel and stably expressed QTL, and further confirmed in different genetic backgrounds. Our results further demonstrated that *QSns.sau-MC-3D.1* may have greater breeding potential because of its no adverse effect on other agronomic traits compared to *WAPO1*. It has been positively selected during Chinese breeding programs since the 1940s. Taken together, the identification of *QSns.sau-MC-3D.1* offers a promising resource to further increase wheat yield.

Author contributions statement JGZ finished the study and wrote this manuscript. WL participated in field work and analyzed data. YYY, XLX, JJL, and MD helped phenotype measurement and data analysis. YLL, HPT, QX and QTJ did field work and data analysis. GYC, PFQ, YFJ, and GDC collected and analyzed data. YJH, YR, LWT, and LLG helped with data analysis. YLZ revised the manuscript. YMW discussed results and revised the manuscript. JM designed the experiments, guided the entire study, participated in data analysis, wrote, and extensively revised this manuscript. All authors participated in the research and approved the final manuscript.

Data availability All data generated or analyzed during this study are included in this published article and its supplementary information files or from the corresponding authors upon reasonable request.

Declarations

Competing interests The authors have declared that no competing interests exist.

Ethical approval All experiments and data analyses were conducted in Sichuan. All authors contributed to the study and approved the final version for submission. The manuscript has not been submitted to any other journal.

References

Beales J, Turner A, Griffiths S, Snape JW, Laurie DA (2007) A pseudo-response regulator is misexpressed in the photoperiod insensitive *Ppd-D1a* mutant of wheat (*Triticum aestivum* L.). Theor Appl Genet 115:721–733

Boden SA, Cavanagh C, Cullis BR, Ramm K, Greenwood J, Jean Finnegan E, Trevaskis B, Swain SM (2015) *Ppd-1* is a key regulator of inflorescence architecture and paired spikelet development in wheat. Nat Plants 1:14016

Che Y, Song N, Yang Y, Yang X, Duan Q, Zhang Y, Lu Y, Li X, Zhang J, Li X, Zhou S, Li L, Liu W (2018) QTL mapping of six spike and stem traits in hybrid population of Agropyron Gaertn. in multiple environments. Front Plant Sci 9:1442

Chen D, Wu X, Wu K, Zhang J, Liu W, Yang X, Li X, Lu Y, Li L (2017) Novel and favorable genomic regions for spike related traits in a wheat germplasm Pubing 3504 with high grain number per spike under varying environments. J Integr Agric 16:2386–2401

Ding A, Cui F, Li J, Zhao C, Wang X, Wang H (2011) QTL analysis of yield and plant height in wheat. Sci Agron Sin 44:2857–2867

Ding P, Zhou J, Zhao C, Tang H, Mou Y, Tang L, Deng M, Wei Y, Lan X, Ma J (2022) Haplotype, genetic effect, geographical distribution and breeding utilization analysis of the wheat spikelet number regulated gene *WAPO1*. Acta Agron Sinica (chinese Version) 48:2196–2209

Dixon LE, Greenwood JR, Bencivenga S, Zhang P, Boden SA (2018) *TEOSINTE BRANCHED1* regulates inflorescence architecture and development in bread wheat (*Triticum aestivum*). Plant Cell 30:563–581

Du D, Zhang D, Yuan J, Feng M, Ni Z (2021) *FRIZZY PANICLE* defines a regulatory hub for simultaneously controlling spikelet formation and awn elongation in bread wheat. New Phytol 231:814–833

Faris JD, Fellers JP, Brooks SA, Gill BS (2003) A bacterial artificial chromosome contig spanning the major domestication locus *Q* in wheat and identification of a candidate gene. Genetics 164:311–321

Ge M, Yu K, Ding A, Liu G (2022) Input-output efficiency of water-energy-food and its driving forces: spatial-temporal heterogeneity of Yangtze river economic belt, China. Int J Environ Res Public Health 19:1340

Guo Z, Yang Q, Huang F, Zheng H, Sang Z, Xu Y, Zhang C, Wu K, Tao J, Prasanna BM, Olsen MS, Wang Y, Zhang J, Xu Y (2021) Development of high-resolution multiple-SNP arrays for genetic analyses and molecular breeding through genotyping by target sequencing and liquid chip. Plant Commun 2:100230

Huang S, Zhang Y, Ren H, Li X, Zhang X, Zhang Z, Zhang C, Liu S, Wang X, Zeng Q, Wang Q, Singh RP, Bhavani S, Wu J, Han D, Kang Z (2022) Epistatic interaction effect between chromosome 1BL (*Yr29*) and a novel locus on 2AL facilitating resistance to stripe rust in Chinese wheat Changwu 357–9. Theor Appl Genet 135:2501–2513

Jung WJ, Seo YW (2021) Development of subgenome-specific PCR markers in the short arm of wheat and rye chromosome 1 and their utilization in wheat-rye translocation breeding. Euphytica 217:142

Kharabian-Masouleh A, Waters DLE, Reinke RF, Ward R, Henry RJ (2012) SNP in starch biosynthesis genes associated with nutritional and functional properties of rice. Sci Rep 2:557

Kuzay S, Xu Y, Zhang J, Katz A, Pearce S, Su Z, Fraser M, Anderson JA, Brown-Guedira G, DeWitt N, Peters Haugrud A, Faris JD, Akhunov E, Bai G, Dubcovsky J (2019) Identification of a candidate gene for a QTL for spikelet number per spike on wheat chromosome arm 7AL by high-resolution genetic mapping. Theor Appl Genet 132:2689–2705

Li Y, Fu X, Zhao M, Zhang W, Li B, An D, Li J, Zhang A, Liu R, Liu X (2018) A genome-wide view of transcriptome dynamics during early spike development in bread wheat. Sci Rep 8:1–16

Li C, Tang H, Luo W, Zhang X, Mu Y, Deng M, Liu Y, Jiang Q, Chen G, Wang J, Qi P, Pu Z, Jiang Y, Wei Y, Zheng Y, Lan X, Ma J (2020a) A novel, validated, and plant height-independent QTL for spike extension length is associated with yield-related traits in wheat. Theor Appl Genet 133:3381–3393

Li Y-F, Zeng X-Q, Li Y, Wang L, Zhuang H, Wang Y, Tang J, Wang H-L, Xiong M, Yang F-Y (2020b) *MULTI-FLORET SPIKELET 2*, a MYB transcription factor, determines spikelet meristem fate and floral organ identity in rice. Plant Physiol 184:988–1003

Li J, Miao B, Wang S, Dong W, Xu H, Si C, Wang W, Duan S, Lou J, Bao Z (2022) Hiplot: a comprehensive and easy-to-use web service boosting publication-ready biomedical data visualization. Brief Bioinform 23:bbac261

Liu S, Zhou R, Dong Y, Li P, Jia J (2006) Development, utilization of introgression lines using a synthetic wheat as donor. Theor Appl Genet 112:1360–1373

Liu J, Luo W, Qin N, Ding P, Zhang H, Yang C, Mu Y, Tang H, Liu Y, Li W, Jiang Q, Chen G, Wei Y, Zheng Y, Liu C, Lan X, Ma J (2018) A 55 K SNP array-based genetic map and its utilization in QTL mapping for productive tiller number in common wheat. Theor Appl Genet 131:2439–2450

Liu J, Yao Y, Xin M, Peng H, Ni Z, Sun Q (2022) Shaping polyploid wheat for success: Origins, domestication, and the genetic improvement of agronomic traits. J Integr Plant Biol 64:536–563

Luo W, Ma J, Zhou X-H, Sun M, Kong X-C, Wei Y-M, Jiang Y-F, Qi P-F, Jiang Q-T, Liu Y-X, Peng Y-Y, Chen G-Y, Zheng Y-L, Liu C, Lan X-J (2016) Identification of quantitative trait loci controlling agronomic traits indicates breeding potential of Tibetan Semiwild Wheat (*Triticum aestivum* ssp. *tibetanum*). Crop Sci 56:2410–2420

Ma J, Ding P, Liu J, Li T, Zou Y, Habib A, Mu Y, Tang H, Jiang Q, Liu Y, Chen G, Wang J, Deng M, Qi P, Li W, Pu Z, Zheng Y, Wei Y, Lan X (2019) Identification and validation of a major and stably expressed QTL for spikelet number per spike in bread wheat. Theor Appl Genet 132:3155–3167

Ma S, Wang M, Wu J, Guo W, Chen Y, Li G, Wang Y, Shi W, Xia G, Fu D (2021) WheatOmics: a platform combining multiple omics data to accelerate functional genomics studies in wheat. Mol Plant 14:1965–1968

Masoodi KZ, Lone SM, Rasool RS (2021) Chapter 7—GENOMIC DNA extraction from the plant leaves using the CTAB method. Adv Methods Mol Biol Biotechnol 7:37–44

Mo Z, Zhu J, Wei J, Zhou J, Xu Q, Tang H, Mu Y, Deng M, Jiang Q, Liu Y, Chen G, Wang J, Qi P, Li W, Wei Y, Zheng Y, Lan X, Ma J (2021) The 55K SNP-based exploration of QTLs for spikelet number per spike in a tetraploid wheat (*Triticum turgidum* L.) population: Chinese Landrace "Ailanmai" × Wild Emmer. Front Plant Sci 12:732837

Seetharam AS, Yu Y, Bélanger S, Clark LG, Meyers BC, Kellogg EA, Hufford MB (2021) The Streptochaeta genome and the evolution of the grasses. Front Plant Sci 12:710383

Shukla S, Singh K, Patil RV, Kadam S, Bharti S, Prasad P, Singh NK, Khanna-Chopra R (2015) Genomic regions associated with grain yield under drought stress in wheat (*Triticum aestivum* L.). Euphytica 203:449–467

Singh K, Batra R, Sharma S, Saripalli G, Gautam T, Singh R, Pal S, Malik P, Kumar M, Jan I, Singh S, Kumar D, Pundir S, Chaturvedi D, Verma A, Rani A, Kumar A, Sharma H, Chaudhary J, Kumar K, Kumar S, Singh VK, Singh VP, Kumar S, Kumar R, Gaurav SS, Sharma S, Sharma PK, Balyan HS, Gupta PK (2021) WheatQTLdb: a QTL database for wheat. Mol Genet Genom 296:1051–1056

Smith SE, Kuehl RO, Ray IM, Hui R, Soleri D (1998) Evaluation of simple methods for estimating broad-sense heritability in stands of randomly planted genotypes. Crop Sci 38:1125–1129

Sun C, Zhang F, Yan X, Zhang X, Dong Z, Cui D, Chen F (2017) Genome-wide association study for 13 agronomic traits reveals distribution of superior alleles in bread wheat from the Yellow and Huai Valley of China. Plant Biotechnol J 15:953–969

Wang Y, Hou J, Liu H, Li T, Wang K, Hao C, Liu H, Zhang X (2019) *TaBT1*, affecting starch synthesis and thousand kernel weight, underwent strong selection during wheat improvement. J Exp Bot 70:1497–1511

Yan L, Fu D, Li C, Blechl A, Tranquilli G, Bonafede M, Sanchez A, Valárik M, Yasuda S, Dubcovsky J (2006) The wheat and barley vernalization gene *VRN3* Is an orthologue of *FT*. Proc Natl Acad Sci USA 103:19581–19586

Zhai H, Feng Z, Li J, Liu X, Xiao S, Ni Z, Sun Q (2016) QTL analysis of spike morphological traits and plant height in winter wheat (*Triticum aestivum* L.) using a high-density SNP and SSR-based linkage map. Front Plant Sci 7:1617

Zhang X, Jia H, Li T, Wu J, Nagarajan R, Lei L, Powers C, Kan C-C, Hua W, Liu Z, Chen C, Carver BF, Yan L (2022) *TaCol-B5* modifies spike architecture and enhances grain yield in wheat. Science 376:180–183

Zhao XL, Shi ZY, Peng LT, Shen GZ, Zhang JL (2011) An atypical HLH protein OsLF in rice regulates flowering time and interacts with OsPIL13 and OsPIL15. New Biotechnol 28:788–797

Zheng J, Liu H, Wang Y, Wang L, Chang X, Jing R, Hao C, Zhang X (2014) *TEF-7A*, a transcript elongation factor gene, influences yield-related traits in bread wheat (*Triticum aestivum* L.). J Exp Bot 65:5351–5365

Zhu T, Wang L, Rimbert H, Rodriguez JC, Deal KR, De Oliveira R, Choulet F, Keeble-Gagnère G, Tibbits J, Rogers J, Eversole K, Appels R, Gu YQ, Mascher M, Dvorak J, Luo M-C (2021) Optical maps refine the bread wheat *Triticum aestivum* cv. Chinese Spring Genome Assembly Plant J 107:303–314

Authors and Affiliations

Jieguang Zhou[1,2] · **Wei Li**[1,2] · **Yaoyao Yang**[1,2] · **Xinlin Xie**[1,2] · **Jiajun Liu**[1,2] · **Yanling Liu**[1,2] · **Huaping Tang**[1,2] · **Mei Deng**[1,2] · **Qiang Xu**[1,2] · **Qiantao Jiang**[1,2] · **Guoyue Chen**[1,2] · **Pengfei Qi**[1,2] · **Yunfeng Jiang**[1,2] · **Guangdeng Chen**[3] · **Yuanjiang He**[4] · **Yong Ren**[4] · **Liwei Tang**[5] · **Lulu Gou**[6] · **Youliang Zheng**[1,2] · **Yuming Wei**[1,2] · **Jian Ma**[1,2]

✉ Yuming Wei
ymwei@sicau.edu.cn

✉ Jian Ma
jianma@sicau.edu.cn

[1] State Key Laboratory of Crop Gene Exploration and Utilization in Southwest China, Sichuan Agricultural University, Chengdu, China

[2] Triticeae Research Institute, Sichuan Agricultural University, Chengdu, China

[3] College of Resources, Sichuan Agricultural University, Chengdu, China

[4] Mianyang Academy of Agricultural Science, Crop Characteristic Resources Creation and Utilization Key Laboratory of Sichuan Providence, Mianyang, China

[5] Panzhihua Academy of Agricultural and Forestry Sciences, Panzhihua, China

[6] College of Agronomy, Sichuan Agricultural University, Chengdu, China